Journal homepage http://revistas.unitru.edu.pe/index.php/SSMM

SELECCIONES MATEMÁTICAS
Universidad Nacional de Trujillo
ISSN: 2411-1783 (Online)
2023; Vol. 10(2): 257-272.

Analysis of a delayed mathematical model for tumor-immune cell interactions with Holling type II functional response

Medina-Diaz John

Received, Oct. 07, 2023; *Accepted, Nov. 30, 2023;* *Published, Dec. 27, 2023*

How to cite this article:
Medina-Diaz J. *Analysis of a delayed mathematical model for tumor-immune cell interactions with Holling type II functional response*. Selecciones Matemáticas. 2023;10(2):257–272. http://dx.doi.org/10.17268/sel.mat.2023.02.03

Abstract

In this study, we analyzed a three-dimensional nonlinear differential system considering Holling type II functional response that describes the dynamics of tumor cells, cytotoxic T lymphocytes, and helper T cells, with a single interaction delay. The linear stability of the internal equilibrium point and the presence of the Hopf bifurcation are examined, with the discrete time delay serving as the bifurcation parameter. To demonstrate the rich dynamic behavior of the model, we present numerical simulations with various values of the time delay τ and the attack rate of cytotoxic T lymphocytes on tumor cells (α_1). These simulations exhibit the presence of periodic oscillations and tumor death with survival of the mentioned immune cells, for all α_1 greater than a fixed threshold with or without delay.

Keywords . Cancer, holling functional response, Hopf bifurcation, delay differential equation

1. Introduction. In cancer research, it is crucial to comprehend the convoluted dynamics of the relationship between tumor and anti-tumor factors of the immune response. In simple terms, cancer is a group of more than 100 diseases that develop over time and involve the uncontrolled division of the body cells [1, 26]. Although cancer can develop in virtually any of the body tissues, and each type of cancer has its unique features, the basic processes that produce cancer are quite similar in all forms of the disease such as interruption of normal cell proliferation, differentiation, and cell apoptosis [20, 24]. The perplexing and challenging development of a cancerous tumor involves genetic mutations of normal cells as well as physiological changes within cancer cells, its microenvironment, and the body's defense mechanisms including the immune system [10, 22, 29]. The immune system is a complex network of cells (e.g., white blood cells, especially T lymphocytes, natural killer cells, macrophages), tissues, organs, and the substances (e.g., cytokines, antibodies) they make that help the host fight infections and other diseases as cancer [8]. The lymphocytes usually recognize any foreign cells in the body known as antigens. The resting cells cannot kill the cancer cells but are converted to a special type of T lymphocyte called NK cells or hunting cells. It has been shown experimentally that these immune cells can lyse tumor cells very effectively [16].

To better understand the mechanisms of cancer proliferation and its destruction (i.e., the complex and continuously changing interactions between tumor cells and other components of the tumor microenvironment), researchers around the world developed different kinds of mathematical models in their way [14, 15, 17, 27]. These models have great benefits as they can help to explore, and investigate interactions at different biological scales (e.g., molecular, cellular, and tissues), and to research heterogeneity of cellular dynamics, mutations, and selection [3, 13]. There are numerous reviews of mathematical models of tumor growth and tumor-immune system interactions [14, 6]. There are few reviews that focus on nonspatial models represented by ordinary differential equations (see for example [5, 2, 1, 6]). An ordinary differential

*Departamento de Matemática Pura, Universidad Nacional Mayor de San Marcos, Lima - Perú. **Correspondence author** (john.medina@unmsm.edu.pe).

equation model can involve a single equation for the growth dynamics of the tumor only. If we consider more traits of the tumor microenvironment and the immune system, we note that more complex models have been formulated [6, 18, 27]. Such complexity can be depicted through multi-equation ODE models. These multi-equation models have an advantage as they can explore the emergent properties of the system (such as competition among various components), even when the properties of the individual components are not fully known. To build more realistic models, authors have considered delays in different natural process representations [4, 25, 11]. It is important the consideration of the time delays to explain the time required for the assembly of molecules, differentiation of cell populations, proliferation, etc. [9, 23]. [23] presented a delayed ODE competition model of tumor growth that includes the immune system response and a cycle-phase-specific drug to take into account the cell cycle phase. They showed theoretically and through numerical simulation that periodic solutions may arise through the Hopf bifurcations [23]. [19] discussed cancer self-remission and tumor stability by stochastic approach. Such a model was extended by [12] incorporating discrete time delay to the recruitment of cytotoxic-T-lymphocytes (CTLs) or hunting cells because of the interaction with resting cells or T-helper cells. The authors discussed the existence and stability of equilibrium points, the existence of Hopf-bifurcation, and its direction and stability. Also, [12] assumed the interaction between tumor cells and CTLs as a simple mass-action type.

The subsequent sections of this paper are structured as follows: In Section 2, we present the proposed mathematical model. Section 3 provides an analysis of the model in the absence of delay. We investigate the stability analysis of the non-trivial equilibrium for the model with delay, including the Hopf-bifurcation analysis. In Section 4, we present numerical solutions and illustrations to validate our analytical results. Finally, the paper ends with a brief discussion and conclusion.

2. Model. We propose a non-linear mathematical model considering the state variables, i.e., the density of tumor population $M(t)$, the density of cytotoxic T-lymphocytes or hunting cells $N(t)$ and the density of resting cells $Z(t)$ at any time t in a single tumor-site compartment. As we mentioned above, we modify the model of [12] by considering that the functional response for the tumor cell is Holling-type II. It is assumed that the malignant tumor cells are eliminated by CTLs and resting cells which are directly unable to destroy the tumor cells, but they can be turned into the activated CTLs so that they kill the malignant tumor cells by phagocytosis process. Before stating the problem, let us set some preliminaries:

Let $\tau > 0$ be a fixed number, and $\mathbb{R}^3$ denote the 3-dimensional Euclidean space with norm $\|\cdot\|$. $\mathcal{C} = \mathcal{C}([-\tau, 0], \mathbb{R}^3_{+,0})$, is the Banach space of continuous functions mapping the interval $[-\tau, 0]$ into $\mathbb{R}^3_{+,0}$ with the topology of uniform convergence, where

$$\mathbb{R}^n_{+,0} = \{(x_1, x_2, x_3, ..., x_n) \in \mathbb{R}^n : x_1, x_2, x_3, ..., x_n \geq 0\}.$$

If x is a function belonging to $\mathcal{C}$, then for each fixed $t \in [0, \alpha], 0 \leq \alpha$, the symbol x_t denotes the element of the space $\mathcal{C}$ defined by $x_t(\phi) = x(t+\phi), -\tau \leq \phi \leq 0$. The following system is our deterministic model.

$$\begin{aligned} \frac{dM}{dt} &= rM\Big(1 - \frac{M}{k_1}\Big) - \frac{\alpha_1 M}{\alpha_2 + M} N(t-\tau), \\ \frac{dN}{dt} &= \beta_1 N(t-\tau)Z(t) - dN, \\ \frac{dZ}{dt} &= sZ\Big(1 - \frac{Z}{k_2}\Big) - \beta_2 N(t-\tau)Z. \end{aligned} \tag{2.1}$$

The first equation represents the rate of change of tumor density at any time t. Tumor cells grow in a logistic manner with an intrinsic growth rate r and a carrying capacity k_1. The second term $\frac{\alpha_1 M}{\alpha_2 + M}$ represents the Holling's type-II functional response of the hunting effector-cell to tumor-cell population. The second equation models the change in CTLs population with time t. The delay in obtaining effector functionality after the entry of the remaining T cells into the activation process to be activated hunting T cells is mainly assumed, which is reflected in the cellular interaction modeled in each of the three differential formulations, e.g., $\frac{\alpha_1 M}{\alpha_2 + M} N(t-\tau), \beta_1 N(t-\tau)Z, \beta_2 N(t-\tau)Z$. Add that in the third equation, the natural mortality of resting lymphocytes is contemplated in the logistic growth term. The second factor in the second equation represents the natural death of CTLs at a rate d_1. This last equation describes the dynamics of resting cells at time t, the first term represents its logistic growth, while the death rate of the resting cells is contemplated to be involved in its logistic growth.

The initial condition for the system is given by $M(\theta) = \phi_1(\theta), N(\theta) = \phi_2(\theta), Z(\theta) = \phi_3(\theta), \phi_1(\theta) \geq 0, \phi_2(\theta) \geq 0, \phi_3(\theta) \geq 0$, and $\phi_1(0) > 0, \phi_2(0) > 0, \phi_3(0) > 0$, where $\phi = (\phi_1, \phi_2, \phi_3) \in \mathcal{C}$.

3. Model analysis.

3.1. Analysis of the model without delay. First, we study positivity and existence of equilibria in the general model 2.1, but then we analyze the local stability of such equilibrium points for the system without delay.

3.1.1. Positivity. In this section, we shall demonstrate the positivity of solutions to the system 2.1 by using a theorem which guarantees the system is positive on the interval $[0, +\infty[$.

Lemma 3.1. *Let us consider the general delayed system*

$$\begin{aligned}
\frac{dM}{dt}(t) &= rM(t)\Big(1-\frac{M(t)}{k_1}\Big) - f(M(t))N(t-\tau),\\
\frac{dN}{dt}(t) &= \beta_1 N(t-\tau)g(Z(t)) - dN(t),\\
\frac{dZ}{dt}(t) &= sZ(t)\Big(1-\frac{Z(t)}{k_2}\Big) - \beta_2 N(t-\tau)g(Z(t)),
\end{aligned} \tag{3.1}$$

with $M(0) > 0, N(0) > 0, Z(0) > 0, f \in C(\mathbb{R}, \mathbb{R}), g \in C(\mathbb{R}, \mathbb{R}_{+,0})$ *and* $f(0) \leq g(0) = 0$.

Then, any solution to the system (3.1) with respect to the same above initial conditions exists in the interval $[0, +\infty)$*, and remains nonnegative for all finite time* $t > 0$.

Proof: Let us consider the system (3.1) as $X = (M, N, Z) \in \mathbb{R}^3$ and $\mathcal{F} = (\mathcal{F}_1, \mathcal{F}_2, \mathcal{F}_3) : \mathcal{C} \to \mathbb{R}^3$, where

$$\begin{aligned}
\mathcal{F}_1(X(t)) &= rM(t)\Big(1-\frac{M(t)}{k_1}\Big) - f(M(t))N(t-\tau),\\
\mathcal{F}_2(X(t)) &= \beta_1 N(t-\tau)g(Z(t)) - dN(t),\\
\mathcal{F}_3(X(t)) &= sZ(t)\Big(1-\frac{Z(t)}{k_2}\Big) - \beta_2 N(t-\tau)g(Z(t)).
\end{aligned}$$

We note that $\mathcal{F}_i \in C(\mathcal{C}, \mathbb{R})$ for $i = 1, 2, 3$. Let us fix $t > 0$ such that $X_i(t) = 0$ with $X_t \in \mathcal{C}$, then we easily observe that

$$\mathcal{F}_i \mid_{X_i(t)=0, X_t \in \mathcal{C}} \geq 0 \quad \text{for } i = 1, 2, 3.$$

So, by the result Lemma 2 in [28], we obtain that any solution of $\dot{X} = \mathcal{F}(X_t)$ with $X(t) = X(t, X(0))$ is such that $X(t) \in \mathbb{R}^3_{+,0}, \forall t > 0$.

Theorem 3.1. *Any solution to (2.1), with respect to the same above initial conditions, exists in the interval* $[0, +\infty)$*, and remains nonnegative for all finite time* $t > 0$.

Proof: This follows directly from Lemma 3.1.

3.1.2. Existence of equilibria. In this subsection, we will investigate the biologically feasible non-interior equilibrium points admitted by the model system (2.1). Also, we will explore the interior equilibrium point(s) for (2.1). The following equilibrium points for the problem (2.1) are:

i) trivial equilibrium point $(0, 0, 0)$.

ii) axial equilibrium points $(k_1, 0, 0)$ and $(0, 0, k_2)$.

iii) The $M - Z$ planner equilibrium point $(k_1, 0, k_2)$.

iv) 'Tumor free' equilibrium points

$$(0, \frac{s}{\beta_2}(1 - \frac{d}{\beta_1 k_2}), \frac{d}{\beta_1}).$$

Now, let us display the interior equilibrium points for (2.1). Thus, its interior equilibrium is $(M^*, \frac{s}{\beta_2}(1-\frac{d}{\beta_1 k_2}), \frac{d}{\beta_1})$, where M^* is any value satisfying

$$M^{*2} + (\alpha_2 - k_1)M^* + (\frac{\alpha_1 s}{r\beta_2}(1 - \frac{d}{\beta_1 k_2}) - \alpha_2)k_1 = 0,$$

which implies that (2.1): has exactly one interior equilibrium point if

$\alpha_1 s(\beta_1 k_2 - d) < \alpha_2 r\beta_1\beta_2 k_2$, or $\alpha_2 = k_1 - 2\sqrt{(\frac{\alpha_1 s}{r\beta_2}(1 - \frac{d}{\beta_1 k_2}) - \alpha_2)k_1}$, where in the latter $\alpha_1 s(\beta_1 k_2 - d) > \alpha_2 r\beta_1\beta_2 k_2$,

3.1.3. Local stability analysis. This subsection is done for the local stability analysis of the biologically feasible equilibrium points of the model system (2.1). Since the time delay never changes the number of equilibrium points, so at first, we shall investigate the local stability analysis of the non-delayed system, that is, $\tau = 0$. For the purpose of this, we compute the variational matrix at any arbitrary point (M, N, Z) for the system:

$$\mathcal{J} = \begin{pmatrix} r - 2\frac{rM}{k_1} - f'(M)N & -f(M) & 0 \\ 0 & \beta_1 Z - d & \beta_1 N \\ 0 & -\beta_2 Z & s - 2\frac{sZ}{k_2} - \beta_2 N \end{pmatrix},$$

where

$$f(M) = \frac{\alpha_1 M}{\alpha_2 + M}.$$

For Eq.(2.1), the equilibrium point $(0, 0, 0)$ is always unstable, since the eigenvalues of J_i at $(0, 0, 0)$ are $r > 0, -d, s$. Thus, the equilibrium point $(0, 0, 0)$ is saddle in nature.
At $(k_1, 0, 0)$, the eigenvalues of $\mathcal{J}$ are given by $-r, -d$ and s. Thus, the equilibrium point $(k_1, 0, 0)$ is saddle type.
At $(0, 0, k_2)$, the eigenvalues of $\mathcal{J}$ are given by $r, \beta_1 k_2 - d$ and $-s$. Thus, if $k_2 \neq \frac{d}{\beta_1}$, the equilibrium point $(0, 0, k_2)$ is saddle in nature.
At $(k_1, 0, k_2)$, the eigenvalues of $\mathcal{J}$ are given by $-r, \beta_1 k_2 - d$ and $-s$. Thus, the equilibrium point $(k_1, 0, k_2)$ is stable whenever $k_2 < \frac{d}{\beta_1}$.
At the tumor-free equilibrium point $(0, \frac{s}{\beta_2}(1 - \frac{d}{\beta_1 k_2}), \frac{d}{\beta_1})$, the eigenvalues of $\mathcal{J}$ are $r - f'(0)N^*$, and the other two eigenvalues are the roots of the quadratic equation $\lambda^2 + p_1\lambda + p_2 = 0$, where $p_1 = -s + \frac{2sd}{\beta_1 k_2} + \beta_2 N^*$ and $p_2 = \beta_2 N^* d$. Thus, the equilibrium point $(0, \frac{s}{\beta_2}(1 - \frac{d}{\beta_1 k_2}), \frac{d}{\beta_1})$ will be locally asymptotically stable for the problem iff

$$\frac{\alpha_2 r}{\alpha_1} < N^*.$$

For Eq.(2.1) and at an interior equilibrium point $(M^*, \frac{s}{\beta_2}(1 - \frac{d}{\beta_1 k_2}), \frac{d}{\beta_1})$, the eigenvalues of $\mathcal{J}$ are $r - 2\frac{r}{k_1}M^* - \frac{\alpha_1\alpha_2}{(\alpha_2+M^*)^2}N^*$, and the roots of the quadratic equation $\lambda^2 + p_1\lambda + p_2 = 0$, where $p_1 = -s + \frac{2sd}{\beta_1 k_2} + \beta_2 N^*$ and $p_2 = \beta_2 N^* d$. By classical Routh–Hurwitz criteria, we have the next result for the model 2.1.

Theorem 3.2. *The necessary and sufficient condition for the model system (2.1) to be locally asymptotically stable (in absence of delay, that is, $\tau = 0$) around one of its interior steady states $(M^*, N^*, Z^*) = (M^*, \frac{s}{\beta_2}(1 - \frac{d}{\beta_1 k_2}), \frac{d}{\beta_1})$, is*

$$E: \ \frac{\alpha_1(\alpha_2 + 2M^*)}{(\alpha_2 + M^*)^2} < \frac{r}{N^*},$$

$M^* = \frac{k_1 - d_2 + \sqrt{(k_1 - d_2)^2 - 4c}}{2}$ (if the first condition given in 3.1.2 is satisfied), or $M^* = \sqrt{c}$ (if the second condition given in 3.1.2 is satisfied), where $c = (\frac{\alpha_1 s}{r\beta_2}(1 - \frac{d}{\beta_1 k_2}) - \alpha_2)k_1$.

3.2. Analysis of the model with delay. The equilibria of the model 2.1 with delay are the same as those without delay. Moreover, the equilibria $(0, 0, 0), (k_1, 0, 0), (0, 0, k_2)$ are always unstable. Thus, we will focus only on the stability of an interior equilibrium point $(M^*, \frac{s}{\beta_2}(1 - \frac{d}{\beta_1 k_2}), \frac{d}{\beta_1})$ in presence of delay. In order to see this, we linearize the system (2.1), about the interior steady state $(M^*, \frac{s}{\beta_2}(1 - \frac{d}{\beta_1 k_2}), \frac{d}{\beta_1})$; we get

$$\frac{dX}{dt} = AX(t) + BX(t - \tau), \tag{3.2}$$

where

$$A = \begin{pmatrix} r - 2\frac{rM^*}{k_1} - \frac{\alpha_1\alpha_2}{(\alpha_2 + M^*)^2}N^* & 0 & 0 \\ 0 & -d & \beta_1 N^* \\ 0 & 0 & s - 2\frac{sd}{\beta_1 k_2} - \beta_2 N^* \end{pmatrix},$$

$$B = \begin{pmatrix} 0 & -\frac{\alpha_1 M^*}{\alpha_2 + M^*} & 0 \\ 0 & d & 0 \\ 0 & -\frac{d\beta_2}{\beta_1} & 0 \end{pmatrix},$$

The characteristic equation corresponding to linearized system (3.2) and is

$$det(A + Be^{-\lambda\tau} - \lambda I) = 0, \tag{3.3}$$

respectively.

The stability of equilibrium points is defined by computing the roots of (3.3). For system (2.1) with delay, we can write that the characteristic polynomial evaluated at one of its interior equilibria (M^*, N^*, Z^*) is given by

$$\left(r - 2r\frac{M^*}{k_1} - \frac{\alpha_1\alpha_2}{(\alpha_2 + M^*)^2}N^* - \lambda\right)[\{\lambda^2 + \lambda P_1 + P_2\} + e^{-\lambda\tau}\{\lambda R_1 + R_2\}] = 0, \tag{3.4}$$

where

$$\begin{aligned} P_1 &= d - s + 2\frac{sd}{\beta_1 k_2} + \beta_2 N^*, \\ P_2 &= d(P_1 - d) \\ R_1 &= -d \\ R_2 &= -d(-s + 2\frac{sd}{\beta_1 k_2}) \end{aligned}$$

One root of the aforementioned characteristic polynomial is

$$r - 2r\frac{M^*}{k_1} - \frac{\alpha_1\alpha_2}{(\alpha_2 + M^*)^2}N^*,$$

which is negative if E holds, and the remaining are the roots of the following transcendental equation:

$$L(\lambda, \tau) \equiv P(\lambda) + e^{-\lambda\tau}Q(\lambda) = 0, \tag{3.5}$$

where $P(\lambda) = \lambda^2 + \lambda P_1 + P_2$ and $Q(\lambda) = \lambda R_1 + R_2$. It is the sign of the real parts of the solutions λ of (3.3) which determines the stability of (M^*, N^*, Z^*). So, we proceed to study how the system (2.1) is influenced by the discrete time delay τ, by considering τ as the bifurcation parameter. In order to observe the delay-induced instability, we assume $\lambda = i\psi$ $(\psi > 0)$ is the purely imaginary root of (3.5). Also, the characteristic equation (3.3) of our model system (2.1) has infinitely many solutions, because of its transcendental nature. However, our aim is to find the periodic oscillations of the system (3.5) as the existence of periodic oscillations has an impact on cancer dynamics. So, after substituting $\lambda = i\psi$ in (3.5) and equating the real and imaginary parts, we obtain:

$$-\psi^2 + P_2 = -R_2 cos(\psi\tau) - \psi R_1 sin(\psi\tau), \tag{3.6}$$

$$\psi P_1 = -\psi R_1 cos(\psi\tau) + R_2 sin(\psi\tau). \tag{3.7}$$

Squaring and adding of (3.6) and (3.7), we get

$$(-\psi^2 + P_2)^2 + \psi^2(P_1)^2 = (R_2 cos(\psi\tau) + \psi R_1 sin(\psi\tau))^2 + (\psi R_1 cos(\psi\tau) - R_2 sin(\psi\tau))^2$$

which leads to

$$\psi^4 + D_1\psi^2 + D_2 = 0, \tag{3.8}$$

where

$$D_1 = (P_1)^2 - 2P_2 - (R_1)^2 = (P_1 - d)^2$$
$$D_2 = (P_2)^2 - (R_2)^2$$

Assuming $\psi^2 = u$ we have

$$F(u) = u^2 + uD_1 + D_2 = 0.$$

Thus, by the criterion description from 4.20 in [7], we obtain the following result: If the coefficients D_1, D_2 in $F(u)$ are positive, then the interior equilibrium point (M^*, N^*, Z^*), if it exists, is asymptotically stable for all delay $\tau > 0$ provided it is stable in absence of delay. In other terms, we have the next proposition.

Theorem 3.3. *If*

$$G: \ max\left(\left(1 - \frac{d}{k_2\beta_1 - d}\right), 0\right) < \frac{1}{2}$$

holds, then the interior equilibrium point (M^*, N^*, Z^*) is asymptotically stable for all delay $\tau > 0$ provided its existence and stability in absence of delay.

A simple assumption such that the polynomial Eq. (3.8) will have a nonnegative root is when

$$H: \ 3d < k_2\beta_1.$$

Hence, under the above conditions we imply that there is a unique nonnegative root ψ_0, satisfying the polynomial Eq. (3.8), that is, Eq. (3.5) has a pair of complex roots of the form $i\psi_0$. Solving upon (3.6) and (3.7) and eliminating $sin(\psi\tau)$, we have

$$cos(\psi\tau) = \frac{(R_2 - P_1R_1)\psi^2 - P_2R_2}{(R_2)^2 + (R_1)^2\psi^2}.$$

Then, τ_s corresponding to ψ_0 is

$$\tau_s = \frac{1}{\psi_0} arcos\left(\frac{(R_2 - P_1R_1)\psi_0^2 - P_2R_2}{(R_2)^2 + (R_1)^2\psi_0^2}\right) + \frac{2s\pi}{\psi_0}, \ s = 0, 1, 2, ... \tag{3.9}$$

Without delay, the interior equilibrium point (M^*, N^*, Z^*) is asymptotically stable whenever the condition E_1 holds. Now, based on Butler's Lemma [7], the interior equilibrium point (M^*, N^*, Z^*) remains stable for $\tau < \tau_s$ with $s = 0$.

3.3. Analysis of Hopf Bifurcation. Now, we shall investigate the Hopf bifurcation of the model system (2.1), for which we need to verify the transversality condition

$$\frac{d(\xi)}{d\tau} \mid_{\tau=\tau_s} > 0, \text{ i.e,}$$

$\frac{d(Re\lambda)}{d\tau} \mid_{\tau=\tau_s} > 0$, for $\lambda(\tau) = \xi(\tau) + i\psi(\tau)$. This will designate that there exists at least one eigenvalue with a nonnegative real part for $\tau > \tau_s$. First, we are interested in purely complex roots $\lambda = i\psi_0$ of (3.4). From Equation (3.4) we infer that $\mid P(i\psi_0) \mid = \mid Q(i\psi_0) \mid$, and this defines the possible set of values of ψ_0. Now, we aim to observe the direction of motion of λ as τ is varied. On differentiating (3.5) with respect to τ, we obtain

$$2\lambda\frac{d\lambda}{d\tau} + P_1\frac{d\lambda}{d\tau} + e^{-\lambda\tau}R_1\frac{d\lambda}{d\tau} - \tau e^{-\lambda\tau}(\lambda R_1 + R_2) - \lambda e^{-\lambda\tau}(\lambda R_1 + R_2) = 0$$

Thus,

$$\left(\frac{d\lambda}{d\tau}\right)^{-1} = \frac{e^{\lambda\tau}(2\lambda + P_1)}{\lambda(R_1\lambda + R_2)} + \frac{R_1}{\lambda(R_1\lambda + R_2)} - \frac{\tau}{\lambda}.$$

Since $i\psi_0$ is a simple root of the characteristic equation (3.4), using (3.5) and (3.6) we get at $\lambda = i\psi_0, \tau = \tau_s$

$$\left(\frac{d\lambda}{d\tau}\right)^{-1} |_{\lambda=i\psi_0,\tau=\tau_s} = \frac{d\xi}{d\tau}(i\psi_0, \tau = \tau_s) = \frac{\psi_0^2}{R_1^2\psi_0^4 + R_2^2\psi_0^2} F'(u) \,|_{u=\psi_0^2} .$$

Therefore, $sign(\frac{d\xi}{d\tau}(i\psi_0, \tau = \tau_s))$ is determined by $sign(F'(u) \,|_{u=\psi_0^2})$. So, the transversality condition holds successfully and the system undergoes Hopf bifurcation at $\lambda = i\psi_0, \tau = \tau_s$ by virtue of $D_1 > 0$, i.e., $2d < k_2\beta_1$.

4. Numerical Simulations. In order to fully develop the model, it is crucial to estimate the correct parameter values and initial conditions as they significantly impact the model behavior. We observed that the parameter choices varied significantly among studies, so it was selected values that best suited our deterministic model (2.1), i.e., there were fixed by the author.

$$\alpha_1 = 4, \alpha_2 = 700, r = 1.5, k_1 = 1100, \beta_1 = 0.1, d = 0.35, s = 1, k_2 = 100,$$

$$\beta_2 = 0.05$$

To explore the stability and bifurcation properties of the model system, we conducted a comprehensive set of numerical simulations using the MATLAB function dde23. Specifically, we utilized the parameter values outlined above, along with initial conditions of $M(0) = 4 \times 10^2, N(0) = 5.0, Z(0) = 5$. Through our investigation, we provide a detailed analysis of the local stability properties and Hopf bifurcation characteristics of the system (2.1). Furthermore, our results demonstrate the viability of a range of complex dynamics, e.g., limit cycles, for varying values of the discrete time delay τ regardless of the Holling's type functional response.

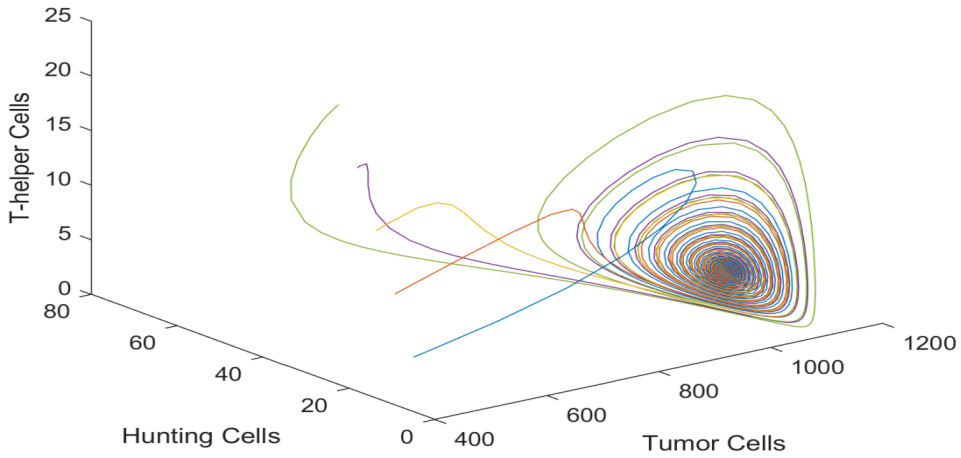

Figure 4.1: 3D phase portrait for our model around the equilibrium point $E^*(1067.98, 19.3, 3.5)$ when $\tau = 0$ alongside the parameter values showed above, for five different initial values.

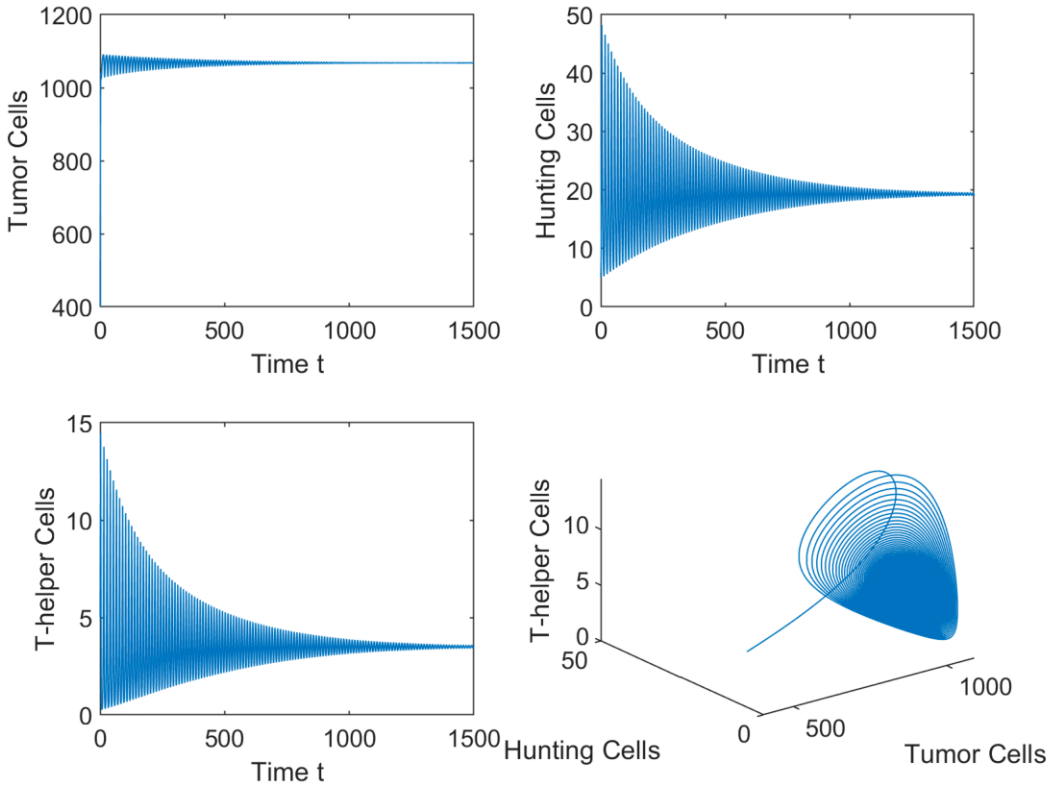

Figure 4.2: The simulation depicts local stability around the unique positive interior equilibrium point $E^*(1067.98, 19.3, 3.5)$ for the delayed system (2.1), with discrete time lag $\tau = 0.09 < \tau_H$ for the initial values $[M(0), N(0), Z(0)] = [400, 5, 5]$, where the other parameter values are same as in Fig. 4.1. In the first row left figure is the time evolution of tumor cells; the first row right figure is the time evolution of CD8+T cells; the second row left figure is the time evolution of T-helper cells; and the second row right figure is the three dimensional phase portrait diagram of the stable interior equilibrium point of 2.1.

For the given parameter values, the system (2.1) has a unique positive interior equilibrium point $E^*(1067.98, 19.3, 3.5)$, respectively, which are stable foci. As observed in Fig. 4.1, plausibly all trajectories that originate within the region of attraction converge towards the interior equilibrium points.

To analyze the impact of different initial densities of tumor cells, activated CD8+T cells, and T-helper cells, we plot the three-dimensional phase portrait diagram of the system described by Eq. (2.1) for various initial conditions [400,5,5]; [405, 10, 10]; [410, 15, 15]; [415, 20, 20]; [420, 25, 25].

In order to confirm our analytical results, we observe that the interior equilibrium point E^* are locally asymptotically stable when $\tau < \tau_H \approx 0.1087$, as shown in Fig. 4.2 for $\tau = 0.09$. The aforementioned figures indicate that when the value of τ is below the critical threshold τ_H, the model system (2.1) approaches the equilibrium state E^*. Specifically, this means that for a delay value of $\tau = 0.09 < \tau_H$, the tumor populations remain under control and may attain a tumor dormant or equilibrium state. However, as the time delay τ surpasses the threshold value τ_H, the interior steady state E^*, undergo a Hopf bifurcation and loses its stability. The transversality condition for Hopf bifurcation is confirmed as $\frac{d(\xi)}{d\tau}\,|_{\tau=\tau_H} \approx 4.644 > 0$. This implies that a stable limit cycle is created around the positive interior equilibrium point E^* at the bifurcation point, resulting in periodic solutions.

The emergence of periodic solutions is of significance in tumor dynamics, since it suggests that tumor levels may oscillate near an equilibrium point in the absence of any treatment. Such behavior has been observed clinically and is commonly referred to as Jeff's Phenomenon [21].

In this study, we conducted numerical simulations to investigate the stability of the delayed model system (2.1) with a given set of parameters. Our results reveal that the stability of the equilibrium points depends on the magnitude of τ. The results depicted in Fig. 4.3 show a Hopf-bifurcating periodic solution around the unique positive equilibrium E^* at $\tau_H \approx 0.1087$.

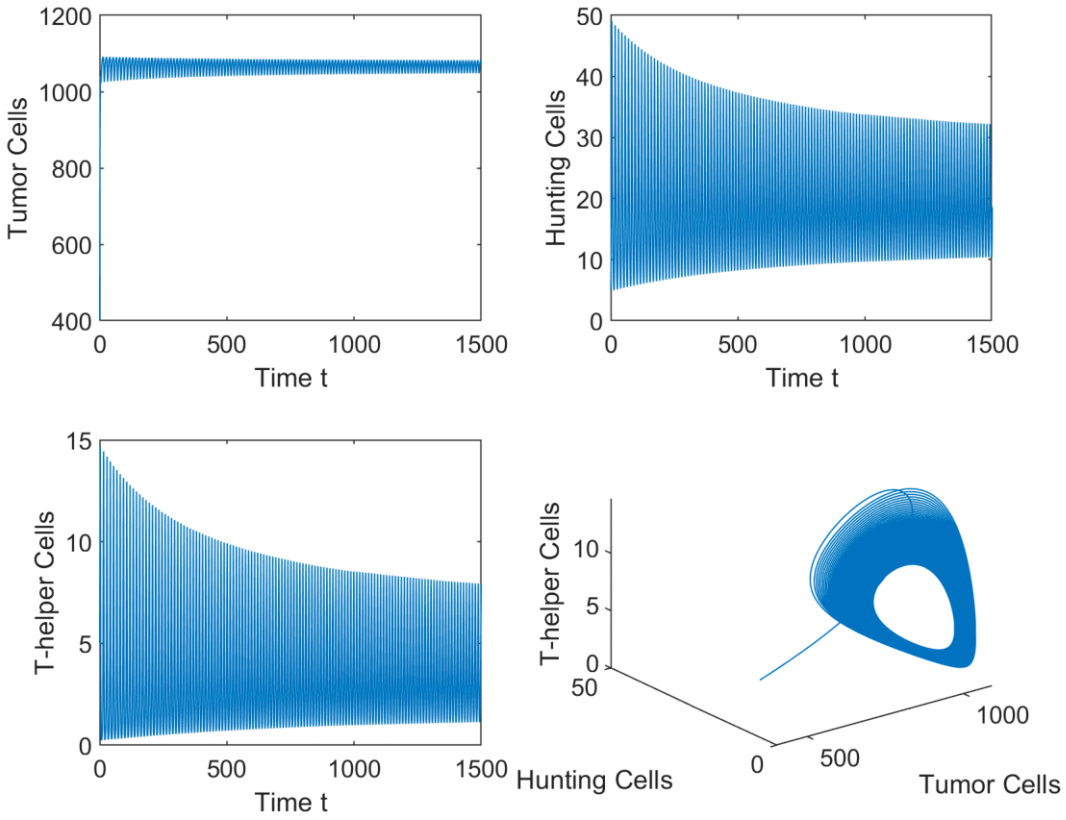

Figure 4.3: Simulation depicts the existence of periodic solution around the unique positive interior equilibrium point $E^*(1067.98, 19.3, 3.5)$ for the delayed system (2.1), when time lag $\tau = 0.1087 \approx \tau_H$ with initial values $[M(0), N(0), Z(0)] = [400, 5, 5]$ where the other parameter values are specified in the Fig. 4.1.

Figures 4.4-4.6 provide insightful two-dimensional phase portrait diagrams showcasing the intricate dynamical behavior of pairwise interactions between tumor cells, CD8+T cells, and T-helper cells, across a range of discrete time delays τ. The first panel of Fig. 4.4 depicts the phase diagrams for $\tau = 0.01$ revealing the stable oscillations of the respective cell populations. Moving on to the second sub-figure of Fig. 4.5, with $\tau = 0.09$, indicates periodic oscillations of the respective cell populations. Finally, Fig. 4.6 showcases the phase diagrams for $\tau = 0.1087$.

In order to gain deeper insights into the significance of the parameter α_1, we analyze the time series solution of model 2.1 (refer to Fig. 4.7, 4.8). Our analysis reveals that an increase in the value of α_1 results not only in an amplification of the magnitude of oscillations exhibited by the tumor cells but also leads to their demise, while the two immune cell populations persist at any value of $\alpha_1 > 56$, irrespective of the delay value.

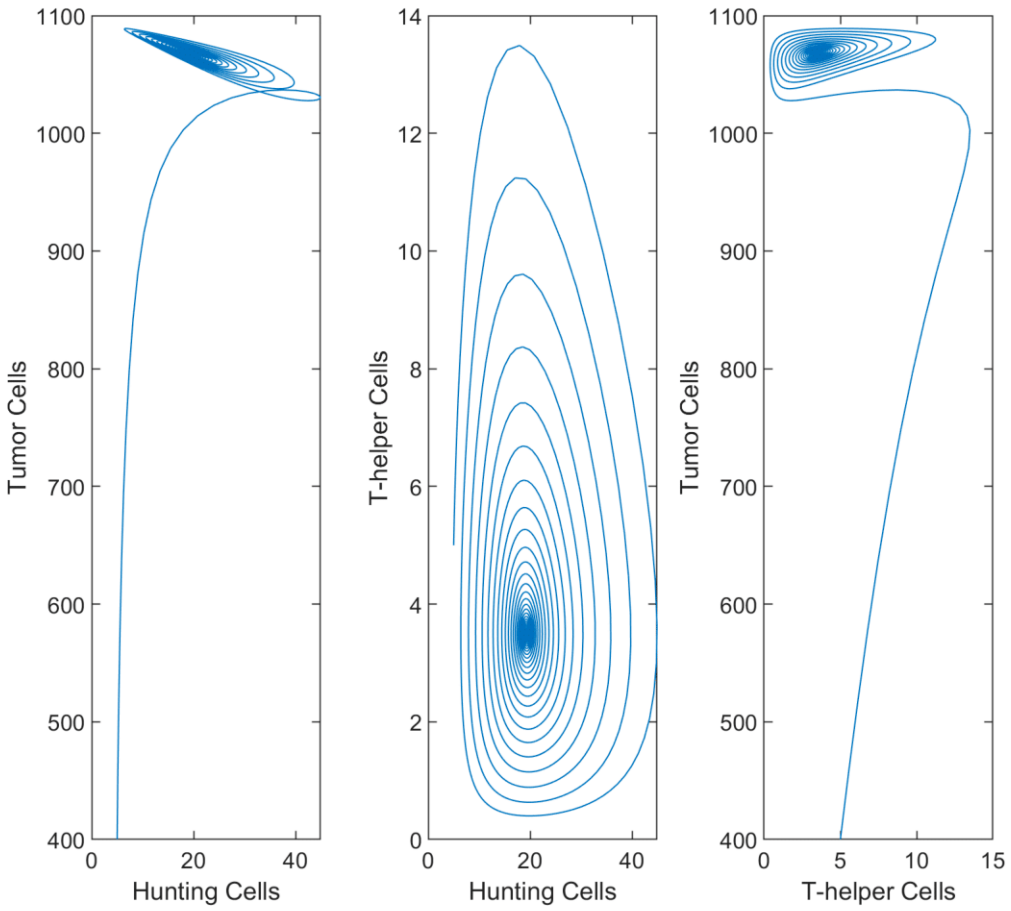

Figure 4.4: Pairwise-interactions between tumor cells, CD8+T cells and T-helper cells at $\tau = 0.01$

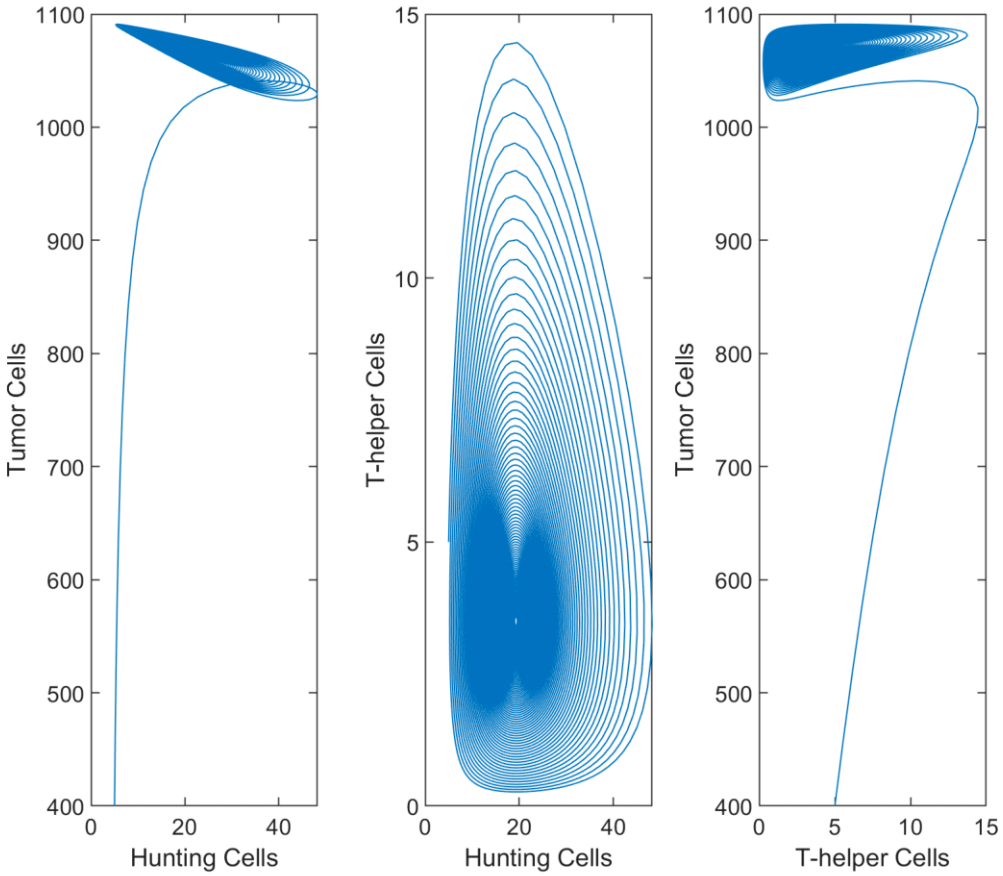

Figure 4.5: Pairwise-interactions between tumor cells, CD8+T cells and T-helper cells at $\tau = 0.09$

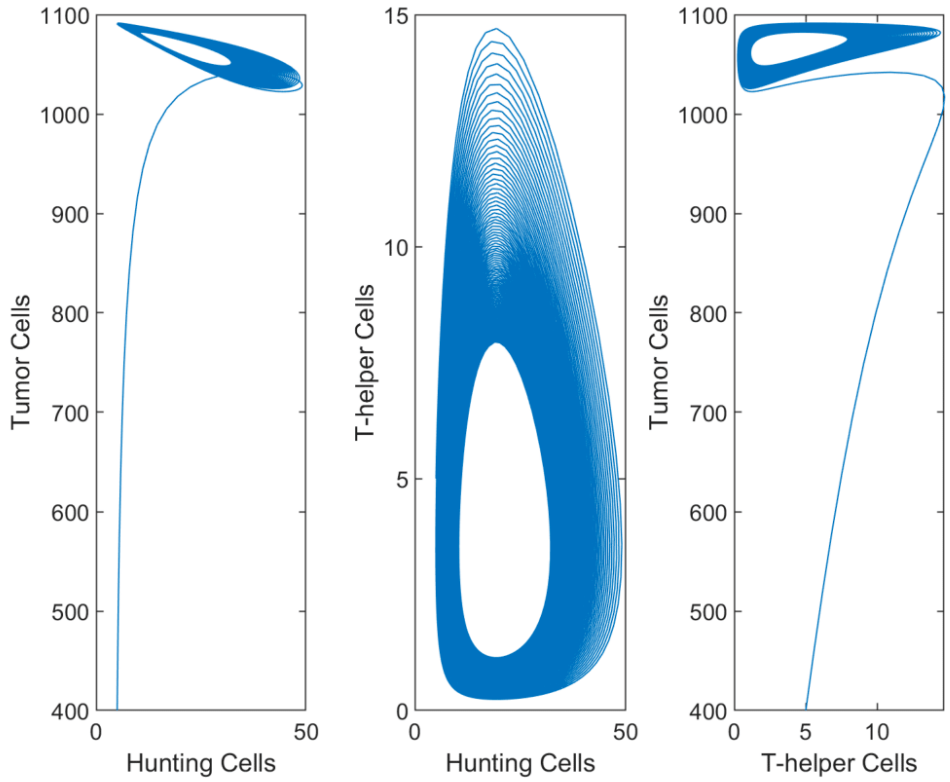

Figure 4.6: Pairwise-interactions between tumor cells, CD8+T cells and T-helper cells at $\tau = 0.1087$

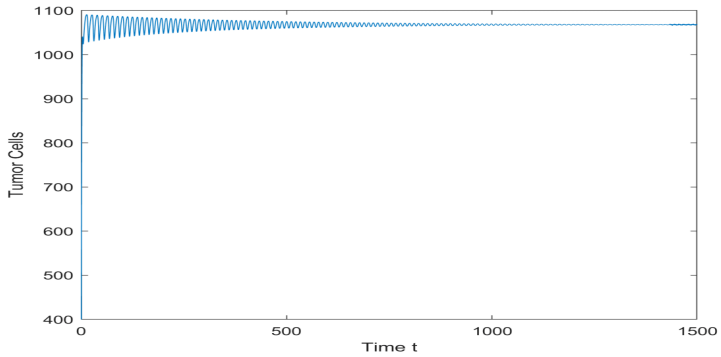

(a) Tumor Population time plot with $\tau = 0.09, \alpha_1 = 4$.

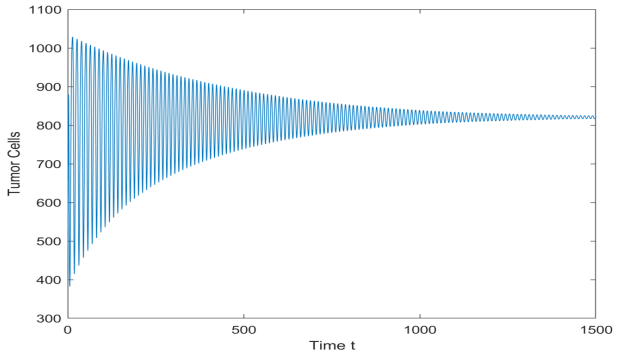

(b) Tumor Population time plot with $\tau = 0.09, \alpha_1 = 30$

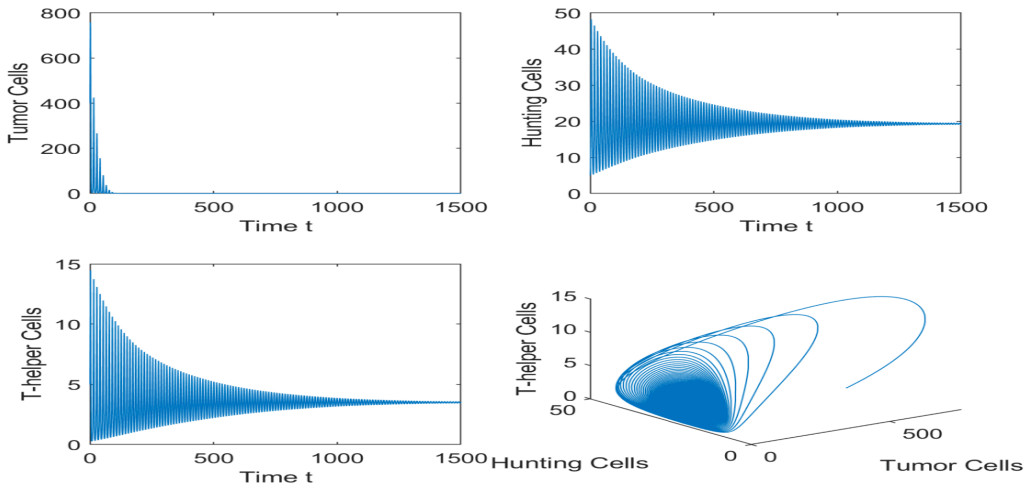

(c) Tumor Population time plot for with $\tau = 0.09, \alpha_1 = 57$

Figure 4.7: Simulation that depicts the oscillating behavior for the delayed system (2.1) emphasizing the tumor dynamics with different α_1 values alongside $\tau = 0.09$, where the other parameter values are the same as in Fig 4.1.

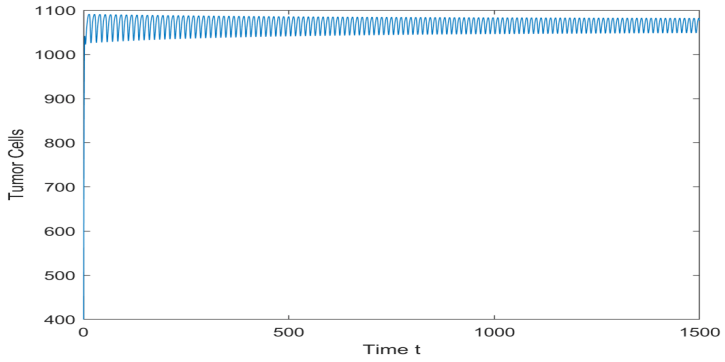

(a) Tumor Population time plot with $\tau = 0.1087, \alpha_1 = 4$.

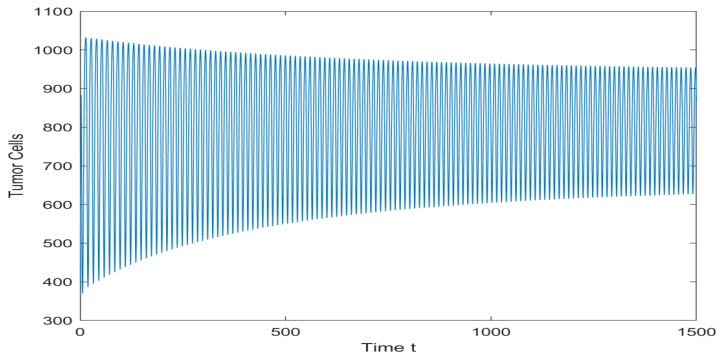

(b) Tumor Population time plot with $\tau = 0.1087, \alpha_1 = 30$

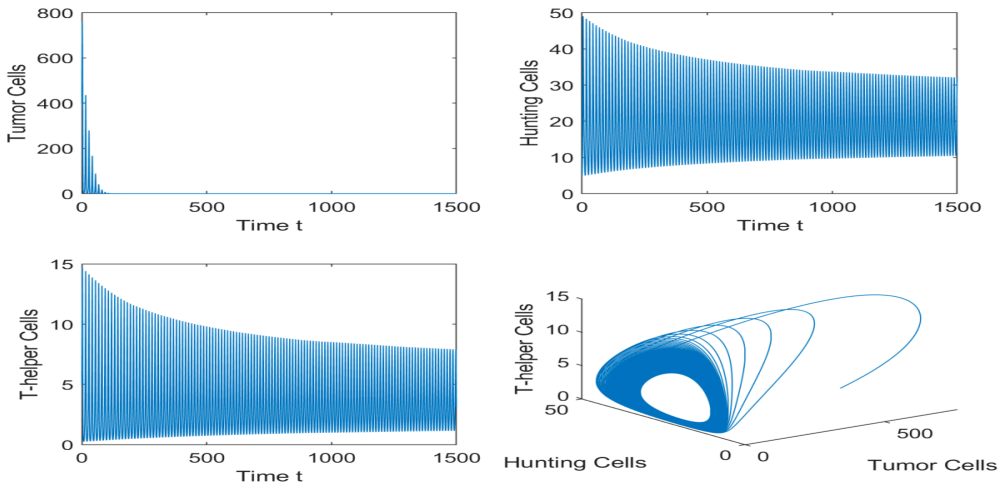

(c) Tumor Population time plot with $\tau = 0.1087, \alpha_1 = 57$

Figure 4.8: Simulation that depicts the oscillating behavior for the delayed system (2.1) emphasizing the tumor dynamics with different α_1 values alongside $\tau \approx \tau_H$, where the other parameter values are the same as in Fig 4.1

5. Discussion. To explore the complex interaction between stimulatory and inhibitory effects on tumor cell growth, we utilize a simple yet effective mathematical model of the immune response. This model comprises a system of three differential equations, incorporating a single time delay for interaction. Indeed, it's important to consider that a highly intricate mathematical model might only result in increased complexity without necessarily offering additional insights into the overall dynamics. Exploring the impact of discrete time delay is not just an intriguing and current area of research; it also contributes significantly to enhancing our comprehension of intricate real-world biological phenomena. We analyse the positive equilibrium point, $E^*(1067.98, 19.3, 3.5)$ of the system (2.1), and examine the nature of the roots of the respective characteristic equation to determine the local asymptotic stability and instability of the steady-state using linear stability analysis. Additionally, we investigate the dynamics of the associated non-delayed system.

In this study, we emphasize the critical role of time delay on the stability of the model system under consideration. Specifically, we show that the stability of the non-negative equilibrium point in the model system (2.1) is determined by the magnitude of the discrete-time lag τ. When the time delay parameter τ is less than a threshold value $\tau_H \approx 0.1087$, the non-negative interior equilibrium E^* is stable. However, the equilibrium point becomes unstable when the time delay τ surpasses its critical magnitude. We observe that a small-scale, periodic solution emerges from the internal equilibrium point E^* as a result of the Hopf bifurcation. We have confirmed that when the time delay parameter τ surpasses the critical value τ_H, the model system (2.1) experiences Hopf bifurcation. Additionally, our calculations determine the magnitud of the discrete time delay parameter τ, providing an indication of the maximum allowable delay length $(\tau \approx 0.1087)$ to maintain the stability of the period limit cycle resulting from the Hopf bifurcation.

Through numerical simulations, we demonstrate that the model system (2.1) experiences Hopf bifurcation when the time delay parameter τ exceeds the threshold value τ_H. Moreover, our numerical simulations indicate that the limit cycle produced through Hopf bifurcation is stable since it attracts the adjacent trajectories and serves as a stable limit set, which can be observed in figure 4.3. Our analytical findings and numerical simulations provide valuable insights into the impact of time delay on the stability of the model system and contribute to a deeper understanding of the tumor-immune interactive dynamics.

6. Conclusions. In the context of tumor-immune interactions, the presence of periodic oscillations holds significant implications for tumor persistence over time and has been observed in other cancer-immune systems. Our mathematical model simulations demonstrate that the oscillatory behavior of the system is highly sensitive to the rate of tumor cell growth, represented by α_1, and the time delay parameter τ. Specifically, when holding other parameters constant and increasing α_1, the magnitude of tumor and Hunting cell oscillations decreases, as shown in Figures 4.7 and 4.8. Moreover, an increase in the value of α_1 to 57 leads to the death of tumor cell populations in system (2.1).

To facilitate the identification of effective treatment strategies for individual patients, it is imperative to investigate the optimal conditions for parameter estimation. Our research endeavors have the potential to offer valuable insights into this area of inquiry. The mathematical model we have employed is general in nature and does not account for the biological intricacies of tumors, including heterogeneity, e.g., altered stroma, stromal interactions; genomic instability, e,g, DNA damage rate of tumor suppressor genes; and tumor growth activation, e.g., stem-like tumor cell dynamics, tumor growth-promoting properties of macrophage migration inhibitory factor. Rather, it is designed to elucidate the nonspecific interactions among different cell populations. Nonetheless, it allows us to reproduce the clinical experiments, such as prolonged latency phases without metastasis, as well as highly invasive tumors that cause rapid metastasis. We trust that the analytical findings and numerical illustrations presented in this study will aid oncologists in their efforts and contribute to the advancement of the tumor immune interactive dynamics field.

Author Contribution . The article has been developed interely for the author JM.

Conflicts of interest. The author declare no conflict of interest.

Acknowledgment. The author would like to thank his parents for their patience in his academic development. The author also would like to thank Roxana Lopez for her general review of the article.

ORCID and License
Medina-Diaz John https://orcid.org/0009-0003-3947-5249

References

[1] Adam, J. A. and Bellomo N., A survey of models for tumor immune system dynamics, Springer Science and Business Media, 1997.

[2] Bajzer Z, Marušić M, Vuk-Pavlović S. Conceptual frameworks for mathematical modeling of tumor growth dynamics. Mathematical and computer modelling. 1996;23(6):31-46.

[3] Bellouquid A, De Angelis E, Knopoff D. From the modeling of the immune hallmarks of cancer to a black swan in biology. Mathematical Models and Methods in Applied Sciences. 2013;23(05):949-978.

[4] Chun-Biao G, Matjaz P, Qing-Yun W. Delay-aided stochastic multiresonances on scale-free FitzHugh–Nagumo neuronal networks. Chinese Physics B. 2010;19(4):040508.

[5] Dullens HFJ, Van Der Tol MWM, De Weger RA, Den Otter W. A survey of some formal models in tumor immunology. Cancer Immunology, Immunotherapy. 1986;23:159-164.

[6] Eftimie R, Bramson JL, Earn DJ. Interactions between the immune system and cancer: a brief review of non-spatial mathematical models. Bulletin of mathematical biology. 2011;73:2-32.

[7] Erbe LH, Freedman HI, Rao VSH. Three-species food-chain models with mutual interference and time delays. Mathematical Biosciences. 1986;80(1):57-80.

[8] Farc O, Cristea V. An overview of the tumor microenvironment, from cells to complex networks. Experimental and therapeutic medicine. 2021;21(1):1-1.

[9] Galach M. Dynamics of the tumor-immune system competition the effect of time delay. Int J Appl Math Comput Sci. 2003;13:395–406.

[10] Grivennikov SI, Greten FR, Karin M. Immunity, inflammation, and cancer. Cell. 2010;140(6):883-899.

[11] Guerrini L, Gori L, Matsumoto A, Sodini M, Zhang Z, Bianca C. Time Delayed Equations as Models in Nature and Society. Discrete Dynamics in Nature and Society. 2016.

[12] Khajanchi S, Nieto JJ. Mathematical modeling of tumor-immune competitive system, considering the role of time delay. Applied mathematics and computation. 2019;340:180-205.

[13] Mahdipour-Shirayeh A, Kaveh K, Kohandel M, Sivaloganathan S. Phenotypic heterogeneity in modeling cancer evolution. PLoS One. 2017;12(10):e0187000.

[14] Mahlbacher GE, Reihmer KC, Frieboes HB. Mathematical modeling of tumor-immune cell interactions. Journal of Theoretical Biology. 2019;469:47-60.

[15] Makhlouf AM, El-Shennawy L, Elkaranshawy HA. Mathematical modelling for the role of CD4+ T cells in tumor-immune interactions. Computational and mathematical methods in medicine. 2020.

[16] North J, Bakhsh I, Marden C, Pittman H, Addison E, Navarrete C, et al. Tumor-primed human natural killer cells lyse NK-resistant tumor targets: evidence of a two-stage process in resting NK cell activation. The Journal of Immunology. 2007;178(1):85-94.

[17] de Pillis LG, Radunskaya AE, Wiseman CL. A validated mathematical model of cell-mediated immune response to tumor growth. Cancer research. 2005;65(17):7950-7958.

[18] Rihan FA, Rihan NF. Dynamics of cancer-immune system with external treatment and optimal control. J. Cancer Sci. Ther. 2016;8(10):257-261.

[19] Sarkar RR, Banerjee S. Cancer self remission and tumor stability–a stochastic approach. Mathematical Biosciences. 2005;196(1):65-81.

[20] Tenen DG. Disruption of differentiation in human cancer: AML shows the way. Nature reviews cancer. 2003;3(2):89-101.

[21] Thomlinson RH. Measurement and management of carcinoma of the breast. Clin Radiol. 1982;33(5):481-93.

[22] Vesely MD, Kershaw MH, Schreiber RD, Smyth MJ. Natural innate and adaptive immunity to cancer. Annual review of immunology. 2011;29:235-271.

[23] Villasana M, Radunskaya A. A delay differential equation model for tumor growth. Journal of mathematical biology. 2003;47:270-294.

[24] Vogelstein B, Kinzler KW. The multistep nature of cancer. Trends in genetics. 1993;9(4):138-141.

[25] Wang Q, Perc M, Duan Z, Chen G. Delay-induced multiple stochastic resonances on scale-free neuronal networks. Chaos: An Interdisciplinary Journal of Nonlinear Science. 2009;19(2).

[26] Weinberg RA. How cancer arises. Scientific American. 1996;275:62–70.

[27] Wilkie KP. A review of mathematical models of cancer–immune interactions in the context of tumor dormancy. Systems biology of tumor dormancy. 2013;201-234.

[28] Yang X, Chen L, Chen J. Permanence and positive periodic solution for the single-species nonautonomous delay diffusive models. Computers and mathematics with applications. 1996;32(4):109-116.

[29] Zamarron BF, Chen W. Dual roles of immune cells and their factors in cancer development and progression. International journal of biological sciences. 2011;7(5):651.